

## Anisotropic Thermal Conductivity of Pyrolytic Graphite

GLEN A. SLACK

General Electric Research Laboratory, Schenectady, New York

(Received March 21, 1962)

The thermal conductivity  $K$  of a bulk sample of pyrolytic graphite has been measured from 3 to 300°K both perpendicular and parallel to the  $c$  axis. Over the whole temperature range below 100°K the thermal conductivity in both directions appears to be limited by the crystallite size. The measured value of  $K_{\perp}$  is 0.72 W/cm deg at 300°K, and  $K_{\perp}$  decreases monotonically to  $1.4 \times 10^{-4}$  W/cm deg at 3°K. The measured anisotropy  $K_{\perp}/K_{\parallel}$  decreases monotonically from 47 at 300°K to 2.5 at 3°K. A theoretical calculation of the anisotropy from the elastic constants yields a value of 2.27 for  $T \leq 1^{\circ}\text{K}$ . A suggestion is offered to explain the rapid rise in the anisotropy with increasing temperature. Previous measurements of  $K_{\perp}/K_{\parallel}$  in natural and commercial graphite samples are much smaller.

### INTRODUCTION

GRAPHITE has an hexagonal crystal structure and has been known for a long time as an anisotropic material.<sup>1</sup> This anisotropy has become important with the recently renewed interest in well-oriented samples of pyrolytic graphite.<sup>2,3</sup> Many of its physical properties, including its thermal conductivity  $K$ , are anisotropic. The present paper reports some recent measurements of the anisotropy in  $K$ , reviews some of the previous measurements of  $K$  on various graphites, and presents a theoretical calculation of the anisotropy of  $K$  for  $T \leq 1^{\circ}\text{K}$ .

Most of the commercial products commonly called carbons and graphites are very poorly oriented agglomerations of carbon atoms in both aromatic (planar) and tetrahedral (diamond-type) bonding.<sup>4,5</sup> Their thermal conductivities both above and below room temperature have been reviewed by various authors.<sup>6-8</sup> Values of  $K$  for these materials at 300°K range from about 0.02 to 4 W/cm deg. The main conclusion of this early work is that  $K$  depends on the size of the graphite crystallites, the perfection of the individual crystallites, the fraction of nongraphitic carbon present between the crystallites, and slightly on the orientation of the crystallites.

Our present interest is in graphite which possesses a high degree of perfection in its crystallite size and orientation, and possesses very little nongraphitic carbon. Pyrolytic graphite is a step in this direction.<sup>9</sup> The  $K$  results on natural and commercial graphite specimens are also of interest. Table I lists most of the available data in the literature<sup>10-14</sup> on the  $K$  of natural

graphite (NG) specimens at 300°K. The values given in Table I are for  $K_{\perp}$  the thermal conductivity, and  $\sigma_{\perp}$  the electrical conductivity, measured in a direction perpendicular to the  $c$  axis of the majority of the graphite crystallites. When available, the anisotropy ratios  $K_{\perp}/K_{\parallel}$  and  $\sigma_{\perp}/\sigma_{\parallel}$  are given. Both of these ratios are greater than unity. The  $K_{\perp}/K_{\parallel}$  ratio for the NG samples varies from 3 to 6, thus indicating the thermal as well as the electrical conductivity is greater along the tightly bound graphite planes than across them where the binding is weak. In highly perfect graphite the carbon-carbon atom distance in the planes is 1.415 Å, while the interplanar spacing is 3.35 Å.

Similar anisotropic behavior is evident in artificially produced commercial graphites (CG). For example, extruded samples have been measured by Powell<sup>15</sup> and by Buerschaper.<sup>16</sup> These samples gave  $K_{\perp}/K_{\parallel}$  ratios at 300°K of 1.15 and 1.6, respectively.

The  $K_{\perp}$  and  $\sigma_{\perp}$  values shown in Table I for the pyrolytic graphite (PG) specimens<sup>6,17-22</sup> are of the same order of magnitude as for the natural graphites and the commercial graphites. However, because of the highly preferred orientation of the crystallites in pyrolytic graphite, the anisotropies  $K_{\perp}/K_{\parallel}$  and  $\sigma_{\perp}/\sigma_{\parallel}$  are much greater. The data available in the present literature<sup>17,18,21</sup> indicate  $K_{\perp}/K_{\parallel}$  ratios for pyrolytic graphite from 95 to 500 at 300°K, and even higher  $\sigma_{\perp}/\sigma_{\parallel}$  ratios.

<sup>11</sup> R. W. Powell, *General Discussion on Heat Transfer* (Institute of Mechanical Engineers, London, 1951), p. 290.

<sup>12</sup> J. Koenigsberger and J. Weiss, *Ann. Physik* **35**, 1 (1911).

<sup>13</sup> E. Jannettaz, *Bull. soc. min. France* **15**, 133 (1892).

<sup>14</sup> A. W. Smith, *Phys. Rev.* **95**, 1095 (1954).

<sup>15</sup> See reference 8, samples 21 and 22.

<sup>16</sup> R. A. Buerschaper, *J. Appl. Phys.* **15**, 452 (1954).

<sup>17</sup> Raytheon Company, *Electronics*, **32**, 124 (1959).

<sup>18</sup> E. F. Keon, Fourth Biennial Conference on Carbon, University of Buffalo, June 15, 1959, (unpublished), Paper No. 74; also *Pyrographite*, High Temperature Materials Department, (Raytheon Company, Waltham, Massachusetts, 1959).

<sup>19</sup> A. R. G. Brown, W. Watt, R. W. Powell, and R. P. Tye, *Brit. J. Appl. Phys.* **7**, 73 (1956); see also reference 7.

<sup>20</sup> M. Pirani and W. Fehse, *Z. Elektrochem.* **29**, 168 (1923).

<sup>21</sup> Raytheon Company, *Sci. American*, **201**, 105 (1959); *Chem. and Eng. News* **37**, 56 (1959). See also *Note added in proof*.

<sup>22</sup> J. C. Bowman, J. A. Krumhansl, and J. T. Meers, *Industrial Carbon and Graphite* (Society of Chemical Industry, London, 1958), p. 52.

<sup>1</sup> A. R. Ubbelohde and F. A. Lewis, *Graphite and Its Crystal Compounds* (Oxford University Press, Oxford, 1960).

<sup>2</sup> W. E. Sawyer, U. S. Patent No. 229,335 (1880).

<sup>3</sup> A. R. G. Brown, A. R. Hall, and W. Watt, *Nature* **172**, 1145 (1953); C. A. Klein, *Revs. Modern Phys.* **34**, 56 (1962).

<sup>4</sup> J. Kakinoki, K. Katuda, T. Hanawa, and T. Ino, *Acta Cryst.* **13**, 171 (1960).

<sup>5</sup> A. W. Smith, *Phys. Rev.* **93**, 952 (1954).

<sup>6</sup> A. W. Smith and N. S. Razor, *Phys. Rev.* **104**, 885 (1956).

<sup>7</sup> R. Berman, *Industrial Carbon and Graphite* (Society of Chemical Industry, London, 1958), p. 42.

<sup>8</sup> R. W. Powell, *Industrial Carbon and Graphite* (Society of Chemical Industry, London, 1958), p. 46.

<sup>9</sup> C. A. Klein and W. D. Straub, *Phys. Rev.* **123**, 1581 (1961).

<sup>10</sup> R. Berman, *Proc. Phys. Soc. (London)* **A65**, 1029 (1952).

TABLE I. Thermal and electrical conductivities and anisotropies of graphite samples at 300°K.

Sample number	Source	$\rho$ (g/cm <sup>3</sup> )	$K_{\perp}$ (W/cm deg)	$\sigma_{\perp}$ (10 <sup>3</sup> $\Omega^{-1}$ cm <sup>-1</sup> )	$K_{\perp}/K_{\parallel}$	$\sigma_{\perp}/\sigma_{\parallel}$	Reference
NG-10	Ceylon <sup>b</sup>	2.17	2.4	1.02	3.2	4.2	10
NG-11	Cumberland	2.21	3.1	1.42	~6	~9	11
NG-12	Ceylon	~2.2	3.6	2.8	...	...	12
NG-13	Ceylon <sup>b</sup>	2.17	4.2	2.9	4.8	6.7	11
NG-14	natural	~2.2	...	...	6.2	...	13
NG-15	Canada	~2.25	4.5	7.7	...	...	14
CG-16	G.L.C.C.	~1.7	1.3	1.07	1.15	1.20	15
CG-17	N.C.C.	~1.6	1.7	1.60	1.6	2.3	16
PG-0	G.E.C.	2.19	0.72	1.85	46	930	<sup>c</sup>
PG-18	N.C.C.	~2.2	1.1	3.3	...	...	6
PG-19	R.C.	~2.1	~2.7	4.4	~95	1000	17
PG-20	R.C.	2.17	4.1	4.4	110	1000	18
PG-21	R.A.E.	2.15	5.8	4.1	...	...	19
PG-22	O.K.	~2.15	>4	~11	...	...	20
PG-23	R.C.	...	...	...	500	1000	21
PG-24	N.C.C.	~2.25	21	14	...	...	22
Single crystal		2.265	~20	25	1000(?)	~2×10 <sup>4</sup>	see text

<sup>a</sup> CG = Commercial graphite, NG = natural graphite, PG = pyrolytic graphite, G.E.C. = General Electric Co., G.L.C.C. = Great Lakes Carbon Corp., N.C.C. = National Carbon Co., O.K. = Osram Konzern, R.A.E. = Royal Aircraft Establishment, and R.C. = Raytheon Company.

<sup>b</sup> both from same block of Ceylon graphite (reference 8).

<sup>c</sup> present data

### PRESENT EXPERIMENT

The present experiment, performed on a pyrolytic graphite sample, was designed to measure both  $K_{\perp}$  and  $K_{\parallel}$  over the temperature range from 3 to 300° K by a technique previously employed.<sup>23</sup> It was hoped that the results would tell whether the anisotropies  $K_{\perp}/K_{\parallel}$ , of the natural graphites (NG) or the pyrolytic graphites (PG), as given in Table I, are more nearly characteristic of well-ordered graphite. The  $K_{\perp}/K_{\parallel}$  anisotropies reported<sup>17,18,21</sup> for pyrolytic graphite are much larger than for any other material known. Some of the largest previous values reported,<sup>24</sup> all on natural minerals, are those for mica-6, brucite [Mg(OH)<sub>2</sub>]-7, slate -8, and slaty-talc-9. Only nonmetallic materials are considered in the present paper. The anisotropy in  $K$  of some metals and semiconductor crystals can be as large<sup>13,23,25</sup> as 5. As can be seen from Table I, the present measurements give  $K_{\perp}/K_{\parallel}=46$ ,  $\sigma_{\perp}/\sigma_{\parallel}=930$  at 300°K. These values agree with the earlier results of other authors on pyrolytic graphite, and indicate that the natural and commercial graphite samples in Table I are, really, nearly isotropic.

### SAMPLE

The present sample (No. 271B, or PG-0 in Table I) of pyrolytic graphite was deposited<sup>26</sup> on a substrate of commercial graphite at 2250°C from a methane atmosphere at a total pressure of 20 mm Hg. Its measured density is 2.194 g/cm<sup>3</sup>. From x-ray measurements the graphite crystallites are thought to be shaped like oblate ellipsoids with rotational symmetry about the  $c$  axis. The minor diameter is  $d_{\parallel}=140$  Å and is parallel

to the  $c$  axis, the major diameter is  $d_{\perp}=280$  Å and lies in the  $a$ - $b$  plane. Macroscopically the sample is composed of columnar bundles of graphite of a maximum diameter of 0.1 cm. The average angular tilt of the crystallites in these columns away from the preferred  $c$ -axis orientation is 22°. Electrical conductivity measurements at 298°K give  $\sigma_{\perp}=1.85\times 10^3 \Omega^{-1} \text{ cm}^{-1}$ ,  $\sigma_{\parallel}=1.98 \Omega^{-1} \text{ cm}^{-1}$ , and hence  $\sigma_{\perp}/\sigma_{\parallel}=930$ . Sound velocity measurements<sup>27</sup> for longitudinal waves at 9.8 Mc/sec and 300°K give  $v_{\perp}=4.7\times 10^5$  cm/sec,  $v_{\parallel}=3.4\times 10^5$  cm/sec for a ratio  $v_{\perp}/v_{\parallel}=1.4$ . The average velocity,  $\frac{1}{3}(2v_{\perp}+v_{\parallel})=4.3\times 10^5$  cm/sec, is in fair agreement with a value of  $4.0\times 10^5$  cm/sec of Wobschall and Hammill<sup>28</sup> on carbon rods. Their results have been linearly extrapolated to a theoretical density of 2.26 g/cm<sup>3</sup>.

The actual pieces, whose  $K$  was measured, were in the shape of solid rods of square cross section cut with the appropriate orientation. The  $K_{\perp}$  sample was 1.9 cm long with a cross-sectional area of 0.14 cm<sup>2</sup>. The  $K_{\parallel}$  sample was 0.7 cm long and had an area of 0.17 cm<sup>2</sup>. They were sound and free from any visible cracks along the (0001) planes. Both pieces were from the same large block of pyrolytic graphite, and came from the same region of the block.

### RESULTS

In Fig. 1 the results of the  $K_{\perp}$  and  $K_{\parallel}$  measurements for the present sample of pyrolytic graphite PG-0 are shown over the temperature range 3 to 300°K. It is quite evident that  $K_{\perp}>K_{\parallel}$  over the whole temperature range, and that the anisotropy ratio  $K_{\perp}/K_{\parallel}$  is a function of temperature. The present  $K_{\perp}$  and  $K_{\parallel}$

<sup>23</sup> G. A. Slack, Phys. Rev. **122**, 1451 (1961).

<sup>24</sup> K. Schulz, Fortschr. Mineral Krist. Petrog. **9**, 221 (1924).

<sup>25</sup> R. W. Powell, Proc. Roy. Soc. (London) **A209**, 525 (1951).

<sup>26</sup> R. J. Diefendorf, J. chim. phys. **57**, 815 (1960).

<sup>27</sup> Courtesy of B. W. Roberts of this Laboratory.

<sup>28</sup> D. Wobschall and H. Hammill, *Fourth Conference on Carbon*, (Pergamon Press, New York, 1960), p. 577.

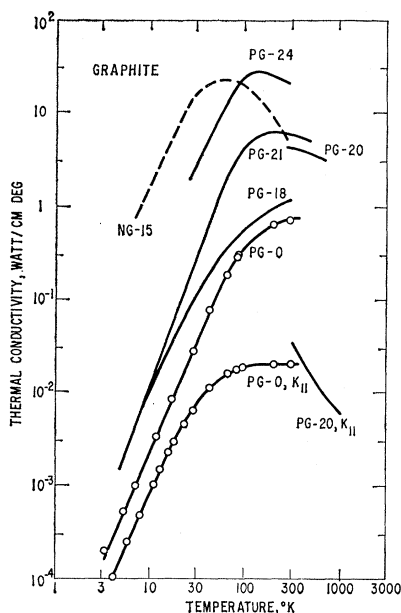


FIG. 1. The thermal conductivity  $K_{\perp}$  (perpendicular to the  $c$  axis) of various samples of pyrolytic graphite (PG) and one sample of natural graphite (NG). The values of  $K_{\parallel}$  (parallel to the  $c$  axis) are also shown for two of the PG samples.

values fall within the range of  $K$  values that have been measured for artificial carbons and graphite (not including pyrolytic graphite) at 300°K, i.e., 0.02 W/cm deg to 4 W/cm deg according to Powell.<sup>8</sup> Other results from the literature for pyrolytic graphite<sup>6,18,19,22</sup> and for a good single flake of natural graphite<sup>14</sup> are also plotted. The values of  $K$  in Fig. 1 at 10°K vary over a range of  $10^3$ . This reflects the wide range of crystallite sizes in the samples studied.

The temperature dependence of  $K$  at low temperatures has been widely discussed in the past.<sup>5,6,14,29,30</sup> For NG-15, PG-18, and PG-24 the value of  $K_{\perp}$  is proportional to  $T^2$ . For PG-21, measured by Berman,  $K_{\perp} \propto T^{2.8}$ . For the present sample PG-0 it was found that  $K_{\perp} \propto T^{2.4}$  and  $K_{\parallel} \propto T^{2.3}$  for  $T < 20^{\circ}\text{K}$ . It does not appear to be true, as Smith and Razor<sup>6</sup> have suggested, that pyrolytic graphite, *per se*, has a  $K \propto T^2$  at low temperatures. The  $T^2$  dependence may only hold for well-oriented and well-annealed pyrolytic graphite samples, such as PG-24 in particular. Furthermore, a  $K \propto T^2$  dependence can only be valid over a limited range of temperatures since at very low temperatures ( $T \leq 1^{\circ}\text{K}$ ) the specific heat capacity  $C$  will vary<sup>31-35</sup> as  $T^3$ . Thus, since the phonon mean free path  $l$  should be

constant in this range,  $K$  should also vary as  $T^3$  at sufficiently low temperatures. These temperatures will be at and below about 1°K according to Komatsu.<sup>32,33</sup>

### SIMPLE ANALYSIS OF THE RESULTS

As a first step, a simple analysis of the thermal conductivity results can be made. A more thorough analysis is introduced later. It is assumed that phonons are by far the dominant carriers of thermal energy in graphite. This has been rediscovered several times<sup>6,12,36</sup> since 1897. Furthermore, the electrons do not affect the mean free path of the phonons.<sup>22</sup> Therefore, only phonons enter the present discussion of  $K$ . At the lowest temperature of 3°K we can compute the phonon mean free path in the graphite planes  $l_1$  from

$$l_1 = 3K_{\perp}/v_1C_T.$$

The numerical values are  $K_{\perp} = 1.4 \times 10^{-4}$  W/cm deg,  $v_1 = 4.7 \times 10^5$  cm/sec (measured), and  $C_T = 1.3 \times 10^{-4}$  J/cm<sup>3</sup> deg. Here  $C_T$  is the total heat capacity of the lattice for large crystallite size natural graphite.<sup>37</sup> The result is  $l_1 \sim 700$  Å, which is to be compared to the x-ray value of 280 Å for  $d_1$ . This agreement is not terribly bad, but it indicates that  $l_1 > d_1$ . Later it will be shown that  $l_1 \approx 10d_1$ .

An approximation to the anisotropy can be calculated from

$$K_{\perp}/K_{\parallel} = l_1v_1C_T/l_{\parallel}v_{\parallel}C_T. \quad (1)$$

Using the measured values of  $d$  and  $v$ , and assuming that  $(l_1/l_{\parallel}) = (d_1/d_{\parallel})$ , the computed anisotropy is 2.8 at 3°K. The measured value of  $K_{\perp}/K_{\parallel}$  at 3°K is 2.5. This is about as far as the simple analysis can be pushed.

### A MORE RIGOROUS ANALYSIS

A detailed knowledge of the lattice vibrational modes of graphite and their dependence on temperature is required in order to understand the magnitude, temperature dependence, and anisotropy of  $K$ . Such an analysis has been carried out in some detail by various authors<sup>33,38</sup> for the total specific heat capacity  $C_T$  as a function of temperature. Let us now restrict the discussion of the thermal conductivity of graphite to the temperature range  $T \leq 1^{\circ}\text{K}$ . In this temperature range the five elastic constants ( $c_{11}$ ,  $c_{12}$ ,  $c_{13}$ ,  $c_{33}$ ,  $c_{44}$ ) are sufficient to describe the modes of vibration. The bending modes of the single graphite sheets, described by Komatsu and Nagamiya<sup>31-33</sup> by the elastic constant  $\kappa$ , are not important in this temperature range. The description of the normal modes at low temperatures has been given in detail by Komatsu.<sup>32</sup> The normal modes can be considered, to a reasonable approximation,

<sup>29</sup> P. G. Klemens, Australian J. Phys. **6**, 405 (1953).

<sup>30</sup> J. E. Hove and A. W. Smith, Phys. Rev. **104**, 892 (1956).

<sup>31</sup> K. Komatsu and T. Nagamiya, J. Phys. Soc. Japan **6**, 438 (1951).

<sup>32</sup> K. Komatsu, J. Phys. Soc. Japan **10**, 346 (1955).

<sup>33</sup> K. Komatsu, J. Phys. Chem. Solids **6**, 380 (1958).

<sup>34</sup> J. A. Krumhansl and H. Brooks, J. Chem. Phys. **21**, 1663 (1953).

<sup>35</sup> J. C. Bowman and J. A. Krumhansl, J. Phys. Chem. Solids **6**, 367 (1958).

<sup>36</sup> L. Cellier, Ann. Physik **61**, 511 (1897).

<sup>37</sup> W. De Sorbo and G. E. Nichols, J. Phys. Chem. Solids **6**, 352 (1958).

<sup>38</sup> A. Yoshimori and Y. Kitano, J. Phys. Soc. Japan **11**, 352 (1956).

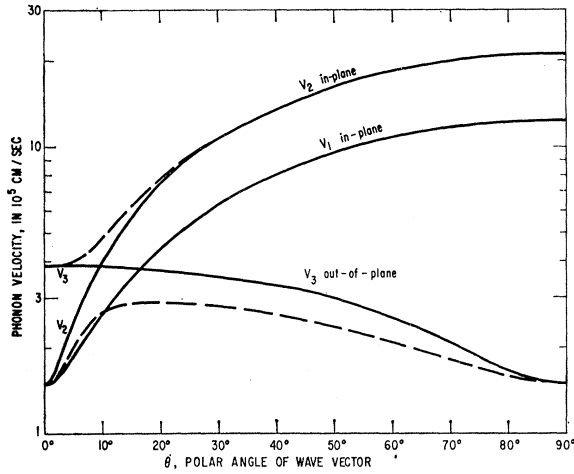


FIG. 2. The velocities  $v_1$ ,  $v_2$ ,  $v_3$  of the three phonon branches as a function of the polar angle  $\theta$ . These velocities are for the temperature range  $T \leq 1^\circ\text{K}$ . The dashed curves between  $v_2$  and  $v_3$  indicate the splitting of these two branches produced by  $c_{33}$  and  $c_{44}$ . This splitting is neglected in the present calculations.

to belong to three separate frequency branches  $\nu_{10}$ ,  $\nu_{20}$ ,  $\nu_{30}$  [see Komatsu,<sup>32</sup> Eq. (9)–(11)]. The propagation velocities  $v$  of these branches in low-temperature, long-phonon wavelength limit are

$$\begin{aligned} v_1^2 &= \rho^{-1}(c_{66} \sin^2\theta + c_{44} \cos^2\theta), \\ v_2^2 &= \rho^{-1}(c_{11} \sin^2\theta + c_{44} \cos^2\theta), \\ v_3^2 &= \rho^{-1}(c_{44} \sin^2\theta + c_{33} \cos^2\theta), \end{aligned} \quad (2)$$

where  $\rho$  is the crystal density,  $c_{66} = (c_{11} - c_{12})/2$ , and  $\theta$  is the polar angle between the propagation vector  $\sigma$  and the  $c$  axis of the graphite crystal. Note that  $|\sigma| = \lambda^{-1}$ , where  $\lambda$  is the phonon wavelength. Figure 2 shows  $v_1$ ,  $v_2$ , and  $v_3$  as a function of  $\theta$  using  $\rho = 2.265$  g/cm<sup>3</sup>.

Since graphite has an hexagonal crystal structure, the velocities in Eq. (2) are independent of the azimuthal angle  $\phi$ . The notation here is related to that of Komatsu<sup>31–33</sup> by the equalities  $c_{11} = \rho v_1^2$ ,  $c_{66} = \rho v_2^2$ ,  $c_{44} = \rho \zeta$ ,  $c_{33} = \rho(\mu c)^2$ .

The vibration characterized by  $\nu_{10}$  and  $v_1$  is a purely transverse branch in which the atomic displacements lie within the graphite sheets. The  $\nu_{20}$ ,  $v_2$  and  $\nu_{30}$ ,  $v_3$  vibrations are, in the strict sense, both mixtures of two other strictly separated branches. This point is discussed later. For the present purposes no significant error is made if the  $\nu_{20}$  and  $\nu_{30}$  are considered as distinct and separate branches. Then the atomic displacements for the  $\nu_{20}$  branch lie nearly in the plane of the graphite sheets for most values of  $\theta$ . By contrast, the displacements for the  $\nu_{30}$  branch lie nearly along the  $c$  axis for most values of  $\theta$ . The  $\nu_{10}$  and  $\nu_{20}$  branches are called the “in-plane” vibrations, while  $\nu_{30}$  is called the “out-of-plane” vibration. It will be seen later that the “out-of-plane” vibrations make the largest contribution to both  $K_{\perp}$  and  $K_{\parallel}$  at low temperatures.

### SPECIFIC HEAT CAPACITY

The specific heat capacity for  $T \leq 1^\circ\text{K}$  can be calculated from these three pseudobranches with good precision. Let  $S(\sigma, j)$  be the heat capacity of a particular normal mode of wave vector  $\sigma$ , polarization  $j$ , and frequency  $\nu$ . The values of  $j$  are 1, 2, 3. Once  $\sigma$  and  $j$  are specified, then  $\nu$  is determined.  $S$ , in terms of  $\nu$ , is

$$S(\sigma, j) = k \left( \frac{h\nu}{kT} \right)^2 \frac{e^{h\nu/kT}}{(e^{h\nu/kT} - 1)^2}, \quad (3)$$

where  $k$  is Boltzmann's constant,  $h$  is Planck's constant, and  $T$  is the absolute temperature. The total heat capacity per unit volume  $C$ , of a crystal of volume  $V$ , is given by the sum over all the normal modes

$$C = V^{-1} \sum_{\sigma, j} S(\sigma, j). \quad (4)$$

The number of normal modes per unit volume of  $\sigma$  space for a particular polarization  $j$  is equal to the crystal volume<sup>39</sup>  $V$ . The total number of modes in the crystal is

$$\begin{aligned} N_{\text{tot}} &= \sum_i \int_{\sigma} V d\sigma \\ &= \left[ V \int_0^{\pi} d\phi \right] \sum_i \int_0^{\pi} \left[ \sin\theta d\theta \int_0^{\sigma_{\text{max}}} \sigma^2 d\sigma \right], \end{aligned} \quad (5)$$

and is equal to  $3\mathfrak{N}$ , where  $\mathfrak{N}$  is the number of atoms in the crystal. In order to compute  $C$  we can now integrate over  $\sigma$  space and sum over the three polarizations:

$$C = \left[ \int_0^{2\pi} d\phi \right] \sum_i \int_0^{\pi} \left[ \sin\theta d\theta \int_0^{\sigma_{\text{max}}} S(\sigma, j) \sigma^2 d\sigma \right]. \quad (6)$$

In the low-temperature region the phase and group velocities are equal, and  $v_1\sigma_1 = \nu_{10}$ . It is assumed that  $T$  is sufficiently low so that  $h\nu_{\text{max}} \gg kT$  for all directions of  $\sigma$  and polarizations  $j$ . Then<sup>39</sup>

$$C = 9k \left( \frac{\mathfrak{N}}{V} \right) \left( \frac{T}{\theta_0} \right)^3 \int_0^{\infty} \frac{x^4 e^{-x} dx}{(e^{-x} - 1)^2}, \quad (7)$$

where

$$\frac{1}{\theta_0^3} = \frac{2\pi k^3 V}{9h^3 \mathfrak{N}} \sum_i \left[ \int_0^{\pi} \frac{\sin\theta d\theta}{[v_j(\theta)]^3} \right]. \quad (8)$$

### ELASTIC CONSTANTS

Since the  $v_j$  values depend on the elastic constants  $c_{ij}$ , it is now necessary to substitute numerical values for  $c_{ij}$ . There are several published<sup>32,33,35</sup> estimates of the  $c_{ij}$  values for graphite. See Table II for some examples. In the present development, values approximating those of Komatsu<sup>32,33</sup> are used for  $c_{11}$ ,  $c_{12}$ , and  $c_{33}$ . The value for  $c_{44}$  is calculated from the experimental

<sup>39</sup> M. Born and K. Huang, *Dynamical Theory of Crystal Lattices* (Oxford University Press, Oxford, 1954), p. 63.

TABLE II. The elastic constants of graphite.

Elastic constant	Value in $10^{10}$ dyn/cm <sup>2</sup>			$c_{ij}/c_{44}$ Slack
	Slack	Komatsu <sup>a</sup>	Bowman and Krumhansl <sup>b</sup>	
$c_{11}$	1000	1000	1130	200
$c_{12}$	333	312	282	(200/3)
$c_{66}^c$	333	344	424	(200/3)
$c_{13}$	~(100)	0	?	0 <sup>d</sup>
$c_{33}$	33.3	34.9	≥18	(20/3)
$c_{44}$	5.00	4.05 <sup>e</sup>	2.3	1

<sup>a</sup> See reference 33.<sup>b</sup> See reference 35.<sup>c</sup>  $c_{66} = \frac{1}{2}(c_{11} - c_{12})$ .<sup>d</sup> See text.<sup>e</sup> For Canadian natural graphite.

value of the Debye temperature  $\theta_0$  in the limit as  $T \rightarrow 0^\circ\text{K}$ .

The constant  $c_{13}$  does not appear in Eq. (2) for the  $v_j$  values. Bowman and Krumhansl<sup>35</sup> show how  $c_{13}$  enters the calculation of the  $v_j$ , but they give no estimate for  $c_{13}$ . Baker *et al.*<sup>40</sup> estimate  $c_{13}$  as  $c_{13} \sim 8 \times 10^{11}$  dyn/cm<sup>2</sup>. If the velocity branches were calculated exactly with the use of nonzero values for  $c_{13}$  and  $c_{44}$ , then the crossover of  $v_2(\theta)$  and  $v_3(\theta)$  at  $\theta = 9^\circ 35'$  in Fig. 2 would be eliminated. The resultant two branches would be a "high-velocity branch" with velocities  $3.83 \times 10^5$  cm/sec at  $\theta = 0^\circ$  and  $21.0 \times 10^5$  cm/sec at  $\theta = 90^\circ$ , and a "low-velocity branch" with a velocity of  $1.48 \times 10^5$  cm/sec at both  $\theta = 0^\circ$  and  $90^\circ$ . The  $v_1$  branch would not be affected. These two new branches would not cross in Fig. 2. They would have velocities at  $\theta = 9^\circ 35'$ , respectively, of 1.24 times and 0.69 times the present common velocity of  $3.79 \times 10^5$  cm/sec of  $v_2$  and  $v_3$ . This splitting, indicated by the dashed lines in Fig. 2, would have some effect on the heat capacity and thermal conductivity. However this splitting has been entirely neglected in the present calculation since it is felt that the estimate<sup>40</sup> of  $c_{13}$  is unreliable, and perhaps too high. From here on, it is assumed that  $c_{13} = 0$ . The nonzero value of  $c_{44}$  by itself causes a very small splitting of about 3% in the velocities at the  $9^\circ 35'$  crossover. This, too, is neglected.

A calculation of the integral in Eq. (8) can be made in closed form by using Eq. (2). The result is

$$\theta_0 = \frac{h}{k} \left[ \frac{3\mathcal{N}}{4\pi V} \right]^{\frac{1}{3}} \left[ \frac{c_{44}}{\rho} \right]^{\frac{1}{3}} \left[ \frac{1}{3}(r_1^{-2} + r_2^{-2} + r_3^{-1}) \right]^{-\frac{1}{3}}, \quad (9)$$

where  $r_1 = (c_{66}/c_{44})^{\frac{1}{2}}$ ,  $r_2 = (c_{11}/c_{44})^{\frac{1}{2}}$ ,  $r_3 = (c_{33}/c_{44})^{\frac{1}{2}}$ . The  $r_1^{-2}$ ,  $r_2^{-2}$ , and  $r_3^{-1}$  are the contributions to  $\theta_0$  from the frequency branches  $\nu_{10}$ ,  $\nu_{20}$ , and  $\nu_{30}$ , respectively. Equation (9), together with Table II, shows that  $\theta_0$  is determined mainly by  $c_{44}$  and  $c_{33}$ , which enter  $\theta_0$  from  $\nu_{30}$ . From Eq. (9) it is evident that the ratios ( $c_{ij}/c_{44}$ ) are important in determining  $\theta_0$ . These same ratios enter again in the computation of  $K$ . Thus the calculations are much simplified by convenient nu-

merical values for ( $c_{ij}/c_{44}$ ). For this reason the numerical ratios given in the fifth column of Table II were used in all of the computations in the present paper. These ratios agree with the values in the second column of Table II, except for  $c_{13}$ .

The best experimental value<sup>41</sup> for  $\theta_0$  is  $420^\circ\text{K} \pm 10^\circ\text{K}$ . The value of  $c_{44}$  determined from this value of  $\theta_0$ , from the absolute values of the other  $c_{ij}$  given in the second column of Table II, and from Eq. (9) is  $c_{44} = 5.11 \times 10^{10}$  dyn/cm<sup>2</sup>. A value of  $c_{44} = 5.00 \times 10^{10}$  dyn/cm<sup>2</sup> (see Table II) is used throughout the present calculations. This value of  $c_{44}$  corresponds to  $\theta_0 = 417^\circ\text{K}$ , and consequently is quite accurate enough for the present purposes.

### THERMAL CONDUCTIVITY

The computation of the two principal thermal conductivities  $K_{\perp}$  and  $K_{\parallel}$  is similar to that just employed for  $\theta_0$  and, hence,  $C$ . Let  $\mathbf{Q}$  be the net heat flow per unit area per unit time across a plane, where  $\mathbf{s}$  is a unit vector normal to this plane. In the relaxation time approximation in which  $\tau(\boldsymbol{\sigma}, j)$  is the relaxation time for the phonon mode  $(\boldsymbol{\sigma}, j)$ , the value of  $\mathbf{Q}$  is given by

$$\mathbf{Q} = (\mathbf{s}/V) \sum_{\boldsymbol{\sigma}, j} (\mathbf{v}_j \cdot \nabla T) (\mathbf{v}_j \cdot \mathbf{s}) \tau(\boldsymbol{\sigma}, j) S(\boldsymbol{\sigma}, j).$$

Note the summation over all of the modes. Choose a principal direction in the crystal along one of the axes of the thermal conductivity ellipsoid. In graphite these are the  $a$ ,  $b$ , and  $c$  axes. The  $K$  along the  $a$  axis is the same as that along the  $b$  axis. For a principal axis  $\mathbf{s}$  lies along this axis and is parallel to  $\nabla T$ . The principal thermal conductivity  $K_p$  in the direction  $\mathbf{s}$  is

$$K_p = \sum_j \int_{\boldsymbol{\sigma}} (\mathbf{v}_j \cdot \mathbf{s})^2 \tau(\boldsymbol{\sigma}, j) S(\boldsymbol{\sigma}, j) d\boldsymbol{\sigma}. \quad (11)$$

In the pyrolytic graphite sample which was measured, the phonon mean free path  $l$  is determined by boundary scattering at the crystallite interfaces over the whole temperature range below about  $100^\circ\text{K}$ . Thus

$$\tau(\boldsymbol{\sigma}, j) = l/v_j$$

for all values of  $\boldsymbol{\sigma}$  and  $j$ . For the present it is assumed that  $l$  is independent of  $\theta$  and  $\phi$ . For  $K_{\parallel}$ , i.e., along the  $c$  axis,  $\mathbf{v}_j \cdot \mathbf{s} = v_j \cos\theta$ . Similarly for  $K_{\perp}$  one has  $\mathbf{v}_j \cdot \mathbf{s} = v_j \sin\theta \cos\phi$ . The anisotropy of the thermal conductivity enters right here in the term  $\mathbf{v}_j \cdot \mathbf{s}$ . The expression for  $K_{\parallel}$  in the limit of low temperatures is now

$$K_{\parallel} = \left[ lk \left( \frac{kT}{h} \right)^3 \int_0^\infty \frac{x^4 e^x dx}{(e^x - 1)^2} \right] \left[ \int_0^{2\pi} d\phi \right] \times \left[ \sum_j \int_0^\pi \frac{\cos^2\theta \sin\theta d\theta}{[v_j(\theta)]^2} \right], \quad (12a)$$

<sup>40</sup> C. Baker, Y. T. Chou, A. Kelley, *Phil. Mag.* **6**, 1305 (1961).<sup>41</sup> P. Flubacher, A. J. Leadbetter, and J. A. Morrison, *J. Phys. Chem. Solids* **13**, 160 (1960).

while for  $K_{\perp}$  we have

$$K_{\perp} = \left[ lk \left( \frac{kT}{h} \right)^3 \int_0^{\infty} \frac{x^4 e^{-x} dx}{(e^x - 1)^2} \right] \left[ \int_0^{2\pi} \cos^2 \phi d\phi \right] \times \left[ \sum_j \int_0^{\pi} \frac{\sin^3 \theta d\theta}{[v_j(\theta)]^2} \right]. \quad (12b)$$

By using Eqs. (7) and (8) for the heat capacity per unit volume  $C$ , the expressions become

$$K_{\parallel} = lC \left[ \sum_j \int_0^{\pi} \frac{\cos^2 \theta \sin \theta d\theta}{[v_j(\theta)]^2} \right] \left[ \sum_j \int_0^{\pi} \frac{\sin \theta d\theta}{[v_j(\theta)]^3} \right]^{-1}, \quad (13a)$$

$$K_{\perp} = \frac{1}{2} lC \left[ \sum_j \int_0^{\pi} \frac{\sin^3 \theta d\theta}{[v_j(\theta)]^2} \right] \left[ \sum_j \int_0^{\pi} \frac{\sin \theta d\theta}{[v_j(\theta)]^3} \right]^{-1}. \quad (13b)$$

If all of the  $v_j$  were equal to  $\bar{v}_0$  and independent of  $\theta$ , both expressions in Eq. (13) would reduce to

$$K_{\parallel} = K_{\perp} = (l\bar{v}_0 C/3). \quad (14)$$

This is the familiar equation for the thermal conductivity of an isotropic solid in the boundary scattering limit where the phonon mean free path is  $l$ .

The  $\bar{v}_0$  in Eq. (14) can be obtained from the expression for  $\theta_0$  in Eq. (9). Suppose all the  $v_j$  in Eq. (8) were equal to a constant value  $\bar{v}_0$ . This  $\bar{v}_0$  would be given by

$$\bar{v}_0 = \theta_0 (k/h) (4\pi V/3\mathcal{N})^{\frac{1}{3}}.$$

Thus

$$\bar{v}_0 = (c_{44}/\rho)^{\frac{1}{3}} \left[ \frac{1}{3} (r_1^{-2} + r_2^{-2} + r_3^{-1}) \right]^{-\frac{1}{3}}. \quad (15)$$

This yields a calculated value for  $\bar{v}_0$  of  $2.89 \times 10^5$  cm/sec, which is close to the value of  $v_3$  at  $\theta = 45^\circ$ , and is somewhat less than the average longitudinal velocity of  $4.3 \times 10^5$  cm/sec measured on the present sample of pyrolytic graphite. The expressions for  $K_{\parallel}$  and  $K_{\perp}$  in Eq. (13) can now be written in terms of  $\bar{v}_0$  as

$$K_{\parallel} = \left[ \frac{l\bar{v}_0 C}{3} \right] \left[ \frac{1}{2} \sum_j \int_0^{\pi} \left( \frac{\bar{v}_0}{v_j} \right)^2 \sin \theta \cos^2 \theta d\theta \right], \quad (16a)$$

$$K_{\perp} = \left[ \frac{l\bar{v}_0 C}{3} \right] \left[ \frac{1}{4} \sum_j \int_0^{\pi} \left( \frac{\bar{v}_0}{v_j} \right)^2 \sin^3 \theta d\theta \right]. \quad (16b)$$

The six integrals in Eq. (16) can also be evaluated exactly if Eq. (2) is used. The mathematics is simple but tedious. The results for  $K_{\parallel}$  are

$$K_{\parallel} = \left[ \frac{l\bar{v}_0 C}{3} \right] \left[ \frac{1}{3} \left( \frac{1}{r_1^2} + \frac{1}{r_2^2} + \frac{1}{r_3} \right) \right]^{-\frac{2}{3}} \left[ \sum_j R_j \right], \quad (17)$$

where

$$R_1 = \frac{1}{r_1^2 - 1} \left[ \left( \frac{r_1 \ln [r_1 + (r_1^2 - 1)^{\frac{1}{2}}]}{(r_1^2 - 1)^{\frac{1}{2}}} \right) - 1 \right]$$

and

$$R_3 = \frac{1}{r_3^2 - 1} \left[ 1 - \left( \frac{\arctan [(r_3^2 - 1)^{\frac{1}{2}}]}{(r_3^2 - 1)^{\frac{1}{2}}} \right) \right].$$

The expression for  $R_2$  in terms of  $r_2$  is identical to that for  $R_1$  in terms of  $r_1$ . The expression for  $K_{\perp}$  is similar in nature to that for  $K_{\parallel}$ . After substituting the  $c_{ij}/c_{44}$  ratios in the fifth column of Table II into Eq. (17), the values of  $K_{\parallel}$  and  $K_{\perp}$  are

$$K_{\parallel} = [l\bar{v}_0 C/3][0.488], \quad K_{\perp} = [l\bar{v}_0 C/3][0.800]. \quad (18)$$

The calculated anisotropy for  $T \leq 1^\circ\text{K}$  is therefore

$$K_{\parallel}/K_{\perp} = (0.800/0.488) = 1.64.$$

The fractional contributions of each of the three vibrational branches  $\nu_{10}$ ,  $\nu_{20}$ ,  $\nu_{30}$  can be computed for  $K_{\parallel}$  from the ratios  $(R_j/\sum_j R_j)$ , etc. These ratios for  $j=1, 2, 3$  are, respectively, 21.4%, 9.2%, 69.4%. For  $K_{\perp}$  the similar ratios are 3.4%, 1.2%, 95.4%. In both cases the  $\nu_{30}$  branch, corresponding to the "out-of-plane" vibrations,  $j=3$ , produces the dominant contribution.

The anisotropy of 1.64, calculated under the assumption that  $l$  is constant and independent of  $\theta$ , is smaller than the experimental value of 2.5. It is known from x-ray studies of the pyrolytic graphite that the crystallites are about twice as large in diameter in the  $a$ - $b$  plane as they are thick in the  $c$  direction, i.e.,  $d_{\perp} = 2d_{\parallel}$ . Even though the simple analysis showed that  $l_{\perp}$  is not equal to  $d_{\perp}$ , it is still assumed that  $(l_{\perp}/l_{\parallel}) = (d_{\perp}/d_{\parallel})$ . In such a case  $l(\theta) = \bar{l}(2)^{\frac{1}{2}}(1 + 3\cos^2\theta)^{-\frac{1}{2}}$ , i.e., it is assumed that the crystallites are oblate ellipsoids. The  $\bar{l}$  is the diameter of a sphere of the same volume as the mean-free-path ellipsoid. Since  $l_{\perp}/l_{\parallel} = 2$ ,  $\bar{l} = l_{\perp}(2)^{-\frac{1}{2}}$ . It turns out that if one takes for  $l(\theta)$  the simpler expression

$$l(\theta) = \bar{l}(2)^{\frac{1}{2}}(1 + \cos^2\theta)^{-1}, \quad (19)$$

then the integrals in Eq. (11), where  $\tau$  is now a function of  $\theta$ , can be evaluated in closed form. The two different expressions for  $l(\theta)$  given above are identical for  $\theta=0^\circ, 90^\circ$ . The maximum difference between them is only 6% for any value of  $\theta$ . Thus the  $(1 + \cos^2\theta)^{-1}$  equation for  $l(\theta)$  is used. With the ellipsoidal crystallites of graphite:

$$K_{\parallel} = [l\bar{v}_0 C/3][0.403], \quad K_{\perp} = [l\bar{v}_0 C/3][0.913]. \quad (20)$$

The fractional contributions of the  $\nu_{10}$ ,  $\nu_{20}$ ,  $\nu_{30}$  branches are about the same as before. The calculated anisotropy ratio now is 2.27, which compares favorably with the value of 2.5 measured at  $3^\circ\text{K}$ , the lowest temperature reached. The anisotropy as a function of temperature should asymptotically approach the value of 2.27 as  $T$  approaches  $0^\circ\text{K}$ . The experimental ratio of  $K_{\perp}/K_{\parallel}$  for the present sample of pyrolytic graphite (PG-0) in Fig. 3 appears to be approaching a limiting value of 2.2 to 2.4 for  $T \leq 1^\circ\text{K}$ .

The calculated value of the anisotropy is determined mostly by the  $\nu_{30}$  branch, and hence by  $r_3$ . In order to show the effect of a change<sup>35</sup> in  $c_{44}$  on the calculated anisotropy,  $c_{44}$  was both increased and decreased by a factor of 2. All the other  $c_{ij}$  were held constant. The

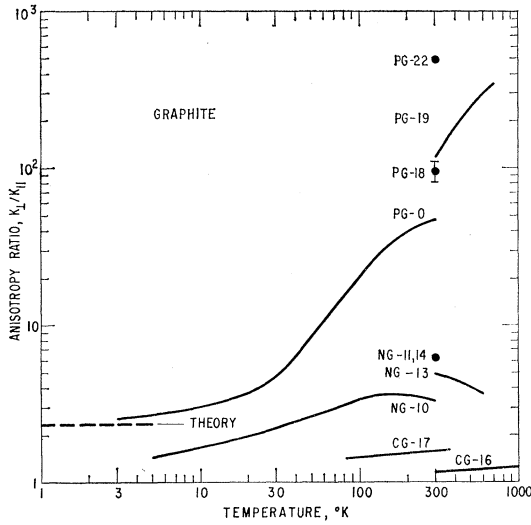


FIG. 3. The measured values of the anisotropy in the thermal conductivity,  $K_1/K_{11}$ , as a function of temperature for samples of pyrolytic (PG), natural (NG), and commercial (CG) graphite. For PG-0 the theory predicts a limiting value of 2.27 for  $T \leq 1^\circ\text{K}$ . This is indicated by the dashed line.

results for the ellipsoidal crystallites are

$$\begin{aligned} c_{44} &= 10.0 \times 10^{10} \text{ dyn/cm}^2, & K_1/K_{11} &= 1.71; \\ c_{44} &= 5.0 \times 10^{10} \text{ dyn/cm}^2, & K_1/K_{11} &= 2.27; \\ c_{44} &= 2.5 \times 10^{10} \text{ dyn/cm}^2, & K_1/K_{11} &= 3.06. \end{aligned} \quad (21)$$

As  $c_{44}$  increases toward  $c_{11}$ ,  $c_{12}$ , etc., the anisotropy decreases. For spherical particles the  $K_1/K_{11}$  values in Eq. (21) should be reduced by  $1.38 \pm 0.01$  for all three cases. The  $5.00 \times 10^{10}$  dyn/cm<sup>2</sup> for  $c_{44}$  derived from  $\theta_0$  gives a better fit to the measured anisotropy in  $K$  than do either of the other values of  $c_{44}$ .

Several other features of the calculated anisotropy should be mentioned. First, the  $(l_1/l_{11})$  ratio of 2 rather than 1 produces an increase in the calculated anisotropy by a factor of only 1.38 instead of 2.00. This reduction in the effect of the crystallite shape is caused by the weighted averaging of  $l(\theta)$  over the interval  $0^\circ \leq \theta \leq 90^\circ$ . Equations (20) and (21) give an anisotropy value in good agreement with the observed value. The effect of allowing  $l$  but not  $v_j$  to be anisotropic can also be evaluated from Eq. (11). This is done by setting all the  $v_j$  equal to  $\bar{v}_0$  and making  $\tau$  a function of  $\theta$ . If Eq. (19) for  $l(\theta)$  is used, then

$$K_{11} = [\frac{1}{3} \bar{l} \bar{v}_0 C][0.811], \quad K_1 = [\frac{1}{3} \bar{l} \bar{v}_0 C][1.079]. \quad (22)$$

Thus the anisotropy  $K_1/K_{11}$  produced by the crystallite shape alone is 1.33. The anisotropy produced by the elastic constants alone is 1.64. The two effects are of comparable importance in determining  $K_1/K_{11}$ . The product  $1.33 \times 1.64 = 2.18$  is somewhat less than the anisotropy of 2.27, which is produced by both effects operating simultaneously.

Next, consider the absolute value of  $\bar{l}$ . At  $1^\circ\text{K}$  the extrapolated value of  $K$  is  $1 \times 10^{-5}$  W/cm deg. With a lattice heat capacity determined from  $\theta_0$  at  $1^\circ\text{K}$  of  $C = 4.95 \times 10^{-6}$  J cm<sup>3</sup> deg, the experimental phonon mean free path is  $\bar{l} = 2000$  Å. This is 10 times larger than the average diameter of the crystallites  $\bar{d} = 220$  Å, as determined by the x-ray line broadening. Since  $\bar{l}$  and  $\bar{d}$  are really determined by much different techniques, it is not surprising that they are unequal. It can be conjectured that the crystallite "boundaries" are not terribly effective in scattering phonons. Perhaps the long-wavelength phonons travel through about 10 crystallites before being scattered. The anisotropy in  $K$  for  $T \leq 1^\circ\text{K}$  is not influenced by the absolute value of  $l_1$  or  $l_{11}$ , providing  $l_1$  and  $l_{11}$  are much less than the diameter ( $\sim 0.5$  cm) of the sample. The  $K_1/K_{11}$  value depends on the ratio  $l_1/l_{11}$ . Similarly  $K_1/K_{11}$  depends on the ratios  $c_{ij}/c_{44}$ , but not on the absolute magnitude of the  $c_{ij}$ . This means that the anisotropy in  $K$  can be calculated with a higher precision than the absolute value  $K$ .

#### ANISOTROPY FOR $T \gg 1^\circ\text{K}$

None of the considerations used so far, in which the graphite crystallites are treated as an elastic continuum yield an anisotropy in  $K$  of the order of 100. By contrast, the experimental values of  $K_1/K_{11}$  at  $300^\circ\text{K}$  for pyrolytic graphite vary from 50 to 500. The marked increase in  $K_1/K_{11}$  as  $T$  increases toward  $300^\circ\text{K}$ , shown in Fig. 3, requires a different explanation. This marked increase is probably caused by the gradual excitation of the plane-bending vibrations considered by Komatsu and Nagamiya<sup>31-33</sup> and by the low heat capacity, low effective temperature, and low velocity of the modes primarily associated with  $c_{44}$  and  $c_{33}$ .

For a very crude analysis at temperatures between  $10^\circ$  and  $100^\circ\text{K}$  let us consider only the  $v_{30}$  vibrational branch. It has just been shown that this branch is responsible for most of the thermal conductivity for  $T \leq 1^\circ\text{K}$ . It is also responsible<sup>32</sup> for most of the heat capacity up to  $90^\circ\text{K}$ . The group velocity<sup>32</sup> for a mode of this branch at  $\theta = 90^\circ$  (i.e., in the graphite planes) is approximately  $v_3(90^\circ) \sim 4\pi\kappa\sigma_x$ , while for  $\theta = 0^\circ$  one obtains  $v_3(0^\circ) \sim (c_{33}/\rho)^{1/2} \cos(\pi c\sigma_x)$ . At, say,  $100^\circ\text{K}$  one can estimate  $\sigma_x \sim \lambda_x^{-1} \sim T/(a_0\theta_x)$ , where  $\theta_x$  is an effective Debye temperature of, maybe,  $1000^\circ\text{K}$ , and  $a_0$  is the lattice constant in the  $x$ - $y$  plane. For  $\lambda_x$  the wavelength of the most numerous phonons at  $100^\circ\text{K}$  has been used, i.e., approximately  $(a_0\theta_x/T)$ . At  $100^\circ\text{K}$   $\sigma_x \sim (2c)^{-1}$ , which makes  $v_3(0^\circ) \sim 0$ . As  $T$  approaches  $0^\circ\text{K}$ , then  $v_3(0^\circ)$  approaches  $(c_{33}/\rho)^{1/2}$ . A weighted  $v_3(0^\circ)$  at  $100^\circ\text{K}$  might be  $\sim \frac{1}{2}(c_{33}/\rho)^{1/2}$ . The anisotropy in  $K$  computed just from  $v_3$  is, crudely,

$$\frac{K_1}{K_{11}} \sim \frac{v_3(90^\circ)}{v_3(0^\circ)} \sim \left[ \frac{20\pi\kappa}{a_0\theta_x} \left( \frac{\rho}{c_{33}} \right)^{1/2} \right] T. \quad (23)$$

This ratio is essentially the ratio of the velocity of the bond-bending, in-plane vibration to the velocity of the compressional, out-of-plane vibration. The anisotropy increases nearly linearly with increasing temperature, as the experimental results in Fig. 3 show for PG-0. If the values given by Komatsu are used, i.e.,  $\kappa=6.11 \times 10^{-3}$  cm<sup>2</sup>/sec,  $a_0=1.415 \times 10^{-8}$  cm,  $(c_{33}/\rho)^{1/2}=3.92 \times 10^5$  cm/sec, then  $K_1/K_{11} \sim 7$  at 100°K. The measured anisotropy at 100°K is 20 for PG-0 in Fig. 3. The temperature  $T_c$  at which the anisotropy in  $K$  changes from that given by Eqs. (18) and (20) to that given by Eq. (23) is, according to Komatsu,<sup>32</sup>

$$T_c = (hc_{44}/4\pi\rho k k).$$

Komatsu<sup>32</sup> gives 2.13°K for  $T_c$ . However, the present value of  $c_{44}$  of  $5.00 \times 10^{10}$  dyn/cm<sup>2</sup> is 6.7 times greater than his. Hence,  $T_c=14^\circ\text{K}$  in the present calculations. The simple elastic theory is, therefore, good for  $T \leq 0.1T_c=1.4^\circ\text{K}$ . The upper limit of 1°K, used throughout the present calculations, appears adequate. A  $T_c$  of 14°K agrees with Fig. 3 where the transition from a temperature independent  $K_1/K_{11}$  to a  $K_1/K_{11} \sim T$  occurs between 10° and 20°K. It should not, however, be assumed that Eq. (23) is at all accurate. A rigorous calculation of  $K_1/K_{11}$  vs  $T$  for  $T > T_c$  would be more complicated than the calculation of the heat capacity.<sup>33,39</sup> Such a calculation of  $K$  has not yet been made.

#### SOME SPECULATIONS

The anisotropy in  $K$  as a function of  $T$  is plotted in Fig. 3 for a number of samples. The results for specimens of natural graphite (NG) and commercial graphite (CG) all show anisotropy ratios  $K_1/K_{11} \leq 6$ . Furthermore the measured anisotropy varies only slowly with temperature. The results on the pyrolytic graphite (PG) samples all indicate that  $K_1/K_{11} \geq 50$  at and above 300°K. It is concluded that the results for the PG samples are more nearly representative of single crystal graphite. All of the present theoretical calculations have been made for an idealized single crystallite of graphite.

The data in Fig. 1 suggest that at 300°K the  $K_{11}$

value of about  $2 \times 10^{-2}$  W/cm deg is determined by phonon-phonon interactions while  $K_1$  for the samples PG- 0, 18, 20, 21 is still limited by the crystallite size. Perhaps the  $K_1$  value for PG-24 at 300°K of 29 W/cm deg is determined by phonon-phonon interactions. Therefore, pyrolytic graphite with a crystallite size of  $> 10^{-3}$  cm might exhibit a  $K_1/K_{11} \simeq 10^3$  at 300°K. This estimated limiting value is included in Table I for comparison with the experimental results. The anisotropy in the electrical conductivity of single crystal graphite at 300°K is even larger than that in  $K$ . It is estimated<sup>42</sup> that for single crystals of graphite  $\sigma_1/\sigma_{11} \simeq 2 \times 10^4$ .

#### CONCLUSIONS

The anisotropy in the thermal conductivity  $K$  of pyrolytic graphite for temperatures  $\leq 1^\circ\text{K}$  lies between 2 and 3. Its exact value is determined by the elastic constants  $c_{ij}$ , and by the ellipsoidal shape of the crystallites. For higher temperatures the bond-bending vibrations of the loosely coupled graphite sheets appear to be responsible for the rapid rise in  $K_1/K_{11}$  for  $T > 14^\circ\text{K}$ . It is suggested that in well-oriented graphite samples with a crystallite size greater than  $\sim 10^{-3}$  cm, the anisotropy in  $K$  might be as large as  $10^3$  at 300°K.

*Note added in proof.* Some more extensive measurements on the thermal conductivity of pyrolytic graphite have recently been made. These confirm the general results shown in Figs. 1 and 3. [See M. G. Holland and C. A. Klein, Bull. Am. Phys. Soc. 7, 191 (1962).]

#### ACKNOWLEDGMENTS

The author would like to thank R. J. Diefendorf and E. R. Stover for the samples of pyrolytic graphite, and for illuminating discussions concerning the nature of pyrolytic graphite. Thanks are extended to J. H. McTaggart for his able assistance in measuring the thermal conductivity, and to B. W. Roberts for his measurements of the sound velocity. Conversations with B. T. Bernstein, G. Dolling, M. G. Holland, and R. E. Jones on graphite are also acknowledged.

<sup>42</sup> R. J. Diefendorf (private communication).